ANNALS of Clinical and Translational Neurology
Open Access
ANA American Neurological Association since 1875

BRIEF COMMUNICATION

Brain iron quantification by MRI in mitochondrial membrane protein-associated neurodegeneration under iron-chelating therapy

Ulrike Löbel[1], Ferdinand Schweser[2,3], Miriam Nickel[4], Andreas Deistung[5], Regine Grosse[6], Christian Hagel[7], Jens Fiehler[1], Angela Schulz[4], Monika Hartig[8], Jürgen R. Reichenbach[5], Alfried Kohlschütter[4] & Jan Sedlacik[1]

[1]Department of Diagnostic and Interventional Neuroradiology, University Medical Center Hamburg-Eppendorf, Hamburg, Germany
[2]Buffalo Neuroimaging Analysis Center, Department of Neurology, School of Medicine and Biomedical Sciences, State University of New York at Buffalo, Buffalo, New York, USA
[3]Buffalo Clinical and Translational Research Center (CTRC), Molecular and Translational Imaging Center, School of Medicine and Biomedical Science, State University of New York at Buffalo, Buffalo, New York, USA
[4]Clinic for Degenerative Brain Diseases, Department of Pediatrics, University Medical Center Hamburg-Eppendorf, Hamburg, Germany
[5]Medical Physics Group, Institute of Diagnostic and Interventional Radiology, Jena University Hospital, Friedrich Schiller University, Jena, Germany
[6]Department of Pediatric Hematology and Oncology, University Medical Center Hamburg-Eppendorf, Hamburg, Germany
[7]Institute of Neuropathology, University Medical Center Hamburg-Eppendorf, Hamburg, Germany
[8]Institute of Human Genetics, Technische Universität München, Munich, Germany

Correspondence
Ulrike Löbel, Martinistrasse 52, 20246 Hamburg, Germany. Tel: +49 (0)40 7410 55598; Fax: +49 (0)40 7410 40114; E-mail: u.loebel@uke.de

Funding Information
This study was supported by Freunde der Kinderklinik UKE Hamburg.

Received: 1 June 2014; Revised: 12 August 2014; Accepted: 16 August 2014

***Annals of Clinical and Translational Neurology* 2014; 1(12): 1041–1046**

doi: 10.1002/acn3.116

Abstract

Therapeutic trials for Neurodegeneration with Brain Iron Accumulation have aimed at a reduction of cerebral iron content. A 13-year-old girl with mitochondrial membrane protein-associated neurodegeneration treated with an iron-chelating agent was monitored by R2 relaxometry, R2* relaxometry, and quantitative susceptibility mapping to estimate the brain iron content. The highly increased brain iron content slowly decreased in the substantia nigra but remained stable for globus pallidus. The estimated iron content was higher by R2* compared to R2 and quantitative susceptibility mapping, a finding not previously observed in the brain of healthy volunteers. A hypothesis explaining this discrepancy is offered.

Introduction

Neurodegeneration with brain iron accumulation (NBIA) is a heterogeneous group of diseases with the unifying feature of excessive iron accumulation in the brain.[1] Recently, mutations in several new genes have been identified and new disease entities were established.[2,3] Currently, no curative treatment is available.

The underlying mechanisms linking iron deposition to neurodegeneration and clinical symptoms still remain unclear for some NBIA subgroups. Recently, a phase II clinical trial in patients with pantothenate kinase-associated neurodegeneration (PKAN) showed markedly reduced brain iron content after treatment with the iron-chelating agent deferiprone.[4] Deferiprone has the ability to mobilize iron from the tissue by donating it to transferrin.[5]

In the current study we used advanced magnetic resonance imaging (MRI) methods to quantitatively asses the brain iron content longitudinally in a patient with mitochondrial membrane protein-associated neurodegeneration (MPAN) treated with deferiprone.

Subject and Methods

Case report

A 13-year-old girl presented with progressive loss of vision over the past six years. Previous testing for the three most

common mtDNA variants associated with Leber's hereditary optic neuropathy had been negative. Recently, a mild cognitive decline had caused her to change to a special school. Concentrating on daily tasks had become difficult for her, and minor gait abnormalities were observed.

The initial MRI performed at our institution showed bilateral optic nerve atrophy and decreased signal intensity on T2-weighted images in globus pallidus and substantia nigra bilaterally (Fig. 1). Consequently, the diagnosis of NBIA was suggested.

Electron microscopic examination of skin biopsy material found no evidence of lysosomal storage but showed morphologically abnormal mitochondria (Fig. S1).

Genetic testing revealed two heterozygous mutations in the *C19orf12* gene (c.l97_199del/p.Gly66del and c.204_214 del/p.Gly69Argfs*10) associated with the clinical phenotype of MPAN.[2,6]

Treatment with deferiprone tablets was initiated at daily doses of 10 mg/kg body weight (four times a day). After 10 months, the medication was gradually increased (5 mg every 6 weeks) to 30 mg/kg under close monitoring of hematological parameters. A low neutrophil count of 1580/μL prompted a decrease in dose to 15 mg/kg, which was tolerated well.

Both parents gave written informed consent consistent with the Declaration of Helsinki in its currently applicable form, which was approved by the local ethics committee.

MRI

Imaging was acquired prior to initiation of therapy, 8, 16, and 24 months later using the same 3 Tesla MR scanner (Skyra; Siemens, Erlangen, Germany) and a standard 20-channel head and neck coil.

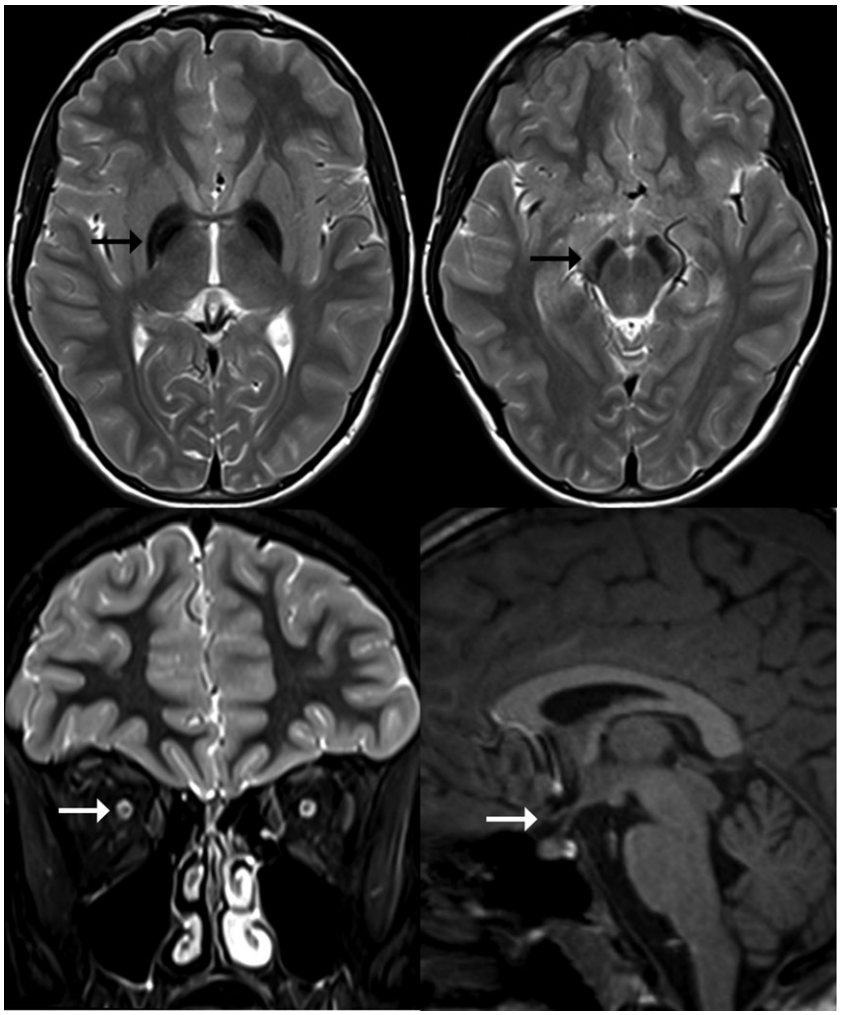

Figure 1. Magnetic resonance imaging of the patient at diagnosis revealed decreased signal intensity of globus pallidus and substantia nigra on T2-weighted images (black arrows) and atrophy of both optic nerves and the optic chiasm (white arrows).

R2 relaxometry was performed by nonlinear fitting of a mono-exponential function to the signal decay obtained by a 2D multi-echo turbo spin-echo sequence with the following parameters: effective TE, 12, 86, and 160 msec; TR, 6580 msec; turbo factor, 6 and 12 msec between refocusing pulses; matrix, 128 × 128; pixel size, 2 × 2 mm^2; slice thickness, 4 mm; gap, 1 mm.

For the calculation of R2* and quantitative susceptibility maps,[7] 3D high-resolution gradient-echo data with the following parameters were used: matrix, 384 × 288 × 64; voxel size, 0.6 × 0.6 × 1 mm^3; TE, 8.5 and 21 msec; TR, 50 msec; flip angle, 17°; bandwidth, 80 Hz/pixel. R2* was calculated by $R2^* = \ln(S_1/S_2)/(TE_2 - TE_1)$, with $S_{1,2}$ denoting the signal measured at the two echoes and $TE_{1,2}$ denoting the corresponding echo times. Single channel gradient-echo phase images were combined as described previously[8] followed by 3D best-path phase unwrapping.[9] The phase images acquired at the different echo times were combined in a noise optimal way[10] and background contributions were eliminated with SHARP (radius: 3 mm, regularization threshold: 0.019).[7] Quantitative susceptibility maps were calculated using the HEIDI algorithm[11] and referenced to CSF.

ROI analysis of R2, R2*, and susceptibility maps was performed by manually defining regions of interest for globus pallidus and substantia nigra in both hemispheres using MRIcro.[12] The ROIs of the left and right hemisphere were combined into a single value for further analysis. Due to partial volume averaging of the 2D sequence used, R2 values of substantia nigra were not reported.

R2 and R2* values were compared with respect to a group of 66 healthy volunteers (36f, 30 m; age range 18–84 years).[13] The tissue iron content for our patient was estimated using the group of healthy volunteers and the age-dependent iron concentrations reported by Hallgren and Sourander.[14]

The quantitative susceptibility mapping (QSM) data were compared to previously published reference values obtained based on a group of 13 deceased subjects (3f; 10 m; age range, 38–81 years) with no history of neurological disorders.[15] Langkammer et al. measured the tissue iron content by inductively coupled plasma mass spectrometry during autopsy. Their values for QSM and tissue iron content were used to extrapolate the brain iron content for our patient.

Results

The patient remained stable clinically and by conventional MRI.

By quantitative MRI at baseline, R2, R2*, and QSM for globus pallidus were 18 ± 2 sec^{-1}, 96 ± 21 sec^{-1} and 0.45 ± 0.14 ppm, respectively. R2* of substantia nigra at baseline was 103 ± 23 sec^{-1} and relative susceptibility was 0.5 ± 0.14. Compared with literature data of controls of a similar age (30 sec^{-1} for globus pallidus, 34 sec^{-1} for substantia nigra), R2* was highly increased.[16] Even compared to healthy elderly controls, R2* and QSM were much higher (Fig. 2). The quantitative results (mean ± standard deviation for all voxels) obtained for globus pallidus and substantia nigra are summarized in the Table S1.

During treatment with deferiprone, R2* and QSM and therefore the iron content decreased significantly over time in substantia nigra (Pearson's correlation coefficient, $R = -0.99$ for both methods with $P = 0.008$ and 0.012, respectively). R2, R2*, and QSM values remained unchanged for globus pallidus (Fig. 3).

A comparison of the extrapolated iron content for globus pallidus showed similar values for R2 relaxometry and QSM, while those obtained by R2* relaxometry were substantially higher. This discrepancy between the estimated iron content by R2* and QSM was also observed for substantia nigra. The estimated iron content for substantia nigra by R2 was not available due to partial volume averaging of the small structure and the 4 mm slice thickness of the 2D MRI sequence for measuring R2. Globus pallidus is a much larger structure; therefore R2 values were likely not affected by partial volume effects as much as within substantia nigra.

Discussion

A patient diagnosed with MPAN showed markedly increased R2* values within globus pallidus and substantia nigra compared to healthy controls of the same age group[16] and even compared to healthy elderly patients.[13] On treatment with the iron-chelating agent deferiprone remained clinically stable and showed slowly decreasing brain iron contents of the substantia nigra estimated by R2* and QSM during an observation period of 24 months. However, iron content in globus pallidus remained stable during the observation period. This is in contrast to previous observations in patients with PKAN, a different subgroup of NBIA, where a marked reduction of the brain iron content was identified already after 6 months of treatment with deferiprone by R2* relaxometry.[4]

Another interesting finding of this report is that the estimated iron content varied depending on the MRI method used. While R2 and QSM showed lower values (range for globus pallidus, 42–53 mg/100 g), the iron content based on R2* was substantially higher (range for globus pallidus, 75–77 mg/100 g). This discrepancy for the iron contents based on R2* and QSM measurements was not previously observed in healthy volunteers or

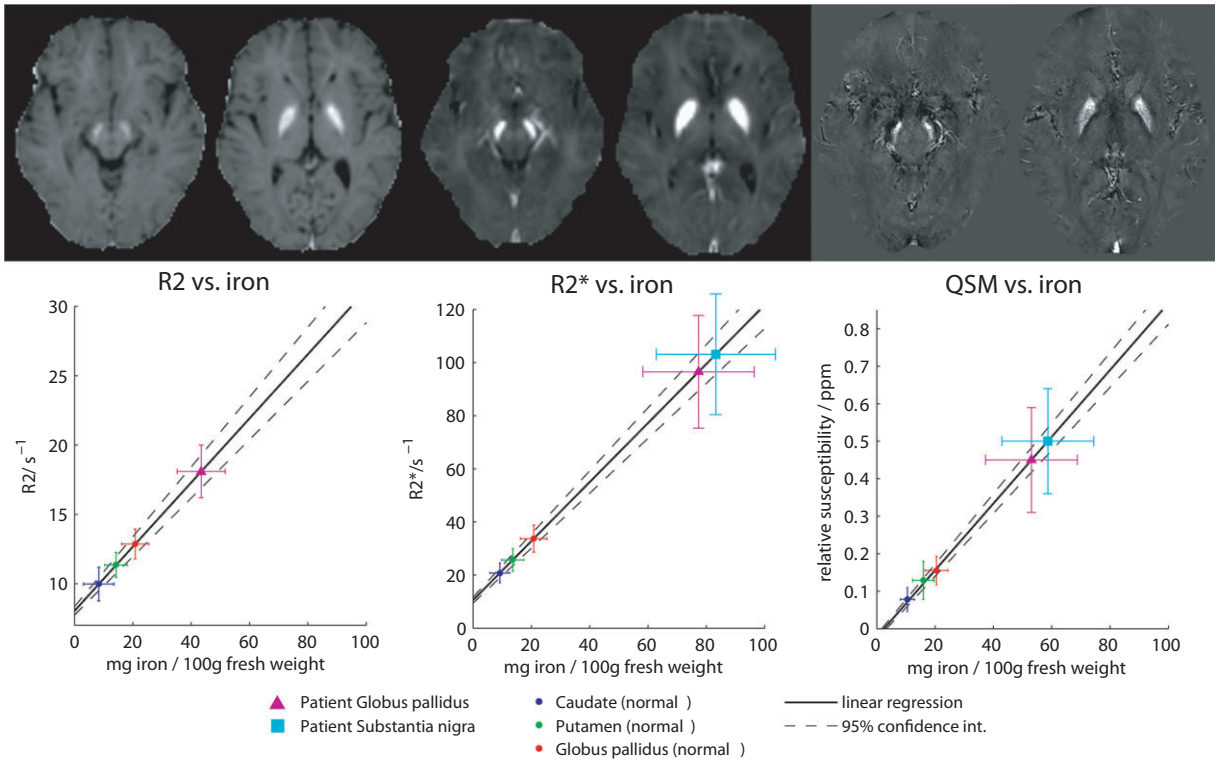

Figure 2. Magnetic resonance imaging of our patient at baseline with respect to cohorts of healthy controls. Above, from left to right: R2, R2*, and QSM maps of substantia nigra and globus pallidus. Below: The graphs depict the measurements for R2, R2*, and QSM as well as the estimated brain iron content of our patient (triangle, square) compared to cohorts of healthy controls (dots). The values obtained and the brain iron content are considerably increased. In contrast to R2 and QSM, the estimated iron content by R2* was higher within globus pallidus. Note: Due to partial volume averaging, R2 and iron content are not available for substantia nigra. QSM, quantitative susceptibility mapping.

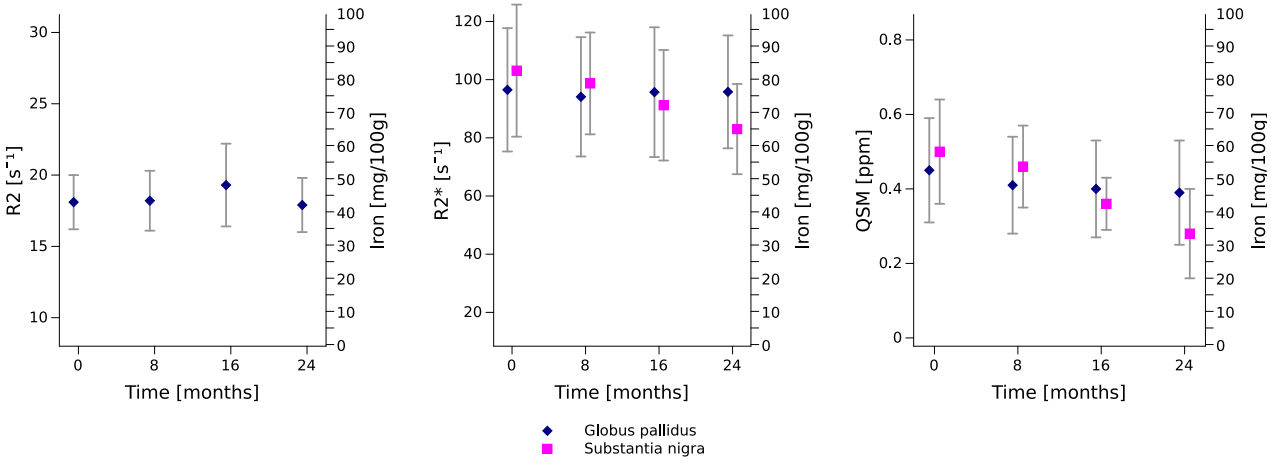

Figure 3. Longitudinal follow-up after initiation of an iron-chelating therapy. The graph depicts the changes observed for R2, R2*, and QSM over time which were significant for substantia nigra only, but not for globus pallidus. QSM, quantitative susceptibility mapping.

deceased subjects without neurological disorders.[13,15] Both articles report a maximum iron content of 25 mg iron/100 g wet tissue for globus pallidus. However, to date no article has directly compared R2* and QSM for the estimation of brain iron content in patients with highly iron overloaded tissue. On the other hand, a curvilinear relationship of R2 with R2*, previously observed in patients with thalassemia and sickle cell disease, has been attributed to a loss of sensitivity of R2 to iron at higher concentrations.[17]

A theoretical explanation for this discrepancy may be that the iron deposits are organized in larger clusters (e.g., confined to a few selected cells) and not diffusely across the tissue. Larger clusters would cause a stronger signal loss in gradient-echo images resulting in higher R2* values compared to a diffuse distribution of the same amount of iron within all cells of the tissue.[13] On the other hand, a diffuse distribution results in a stronger signal loss using spin-echo sequences, causing higher R2 values compared to larger clusters.[17,18]

This would fit histopathological findings in MPAN, which showed densely stained clusters of hemosiderin, but also iron within eosinophilic spheroids, microglia, neuronal concretions, and astrocytes.[2,19] In PKAN, iron is not only present intracellularly, but also diffusely in the neuropil.[20] Hypothetically, this may affect therapeutic strategies in MPAN.

Furthermore, since the magnetic susceptibility is a volume measure, it is insensitive to the organization of the iron deposits.[17,18] Therefore, QSM may provide a method to estimate the brain iron content more independently from tissue microstructure compared to R2 and R2*.

Conclusion

Higher iron content estimates were obtained by R2* relaxometry compared to R2 relaxometry and QSM, suggesting that the iron deposits may be organized in larger clusters (e.g., confined in few selected cells). Further studies are necessary to prove that R2* corresponds more to the iron distribution and QSM is more representative of the iron content.

Acknowledgment

The authors would like to thank Annette Bley MD and Aracelli Meyer-Osores MD for their continued and excellent patient care and many helpful discussions regarding the manuscript. This study was supported by Freunde der Kinderklinik UKE Hamburg. The authors have no conflict of interest to declare with respect to the subject of this manuscript.

Conflict of Interest

Dr. Grosse reports grants from Novartis Oncology Swedish Orphan Biovitrum, personal fees from Novartis Oncology Swedish Orphan Biovitrum, non-financial support from Novartis Oncology Swedish Orphan Biovitrum, outside the submitted work.

References

1. Schneider SA, Hardy J, Bhatia KP. Syndromes of neurodegeneration with brain iron accumulation (NBIA): an update on clinical presentations, histological and genetic underpinnings, and treatment considerations. Mov Disord 2012;27:42–53.
2. Hartig MB, Iuso A, Haack T, et al. Absence of an orphan mitochondrial protein, c19orf12, causes a distinct clinical subtype of neurodegeneration with brain iron accumulation. Am J Hum Genet 2011;89:543–550.
3. Hayflick SJ, Kruer MC, Gregory A, et al. beta-Propeller protein-associated neurodegeneration: a new X-linked dominant disorder with brain iron accumulation. Brain 2013;136(Pt 6):1708–1717.
4. Zorzi G, Zibordi F, Chiapparini L, et al. Iron-related MRI images in patients with pantothenate kinase-associated neurodegeneration (PKAN) treated with deferiprone: results of a phase II pilot trial. Mov Disord 2011;26:1756–1759.
5. Kontoghiorghes GJ. Iron mobilization from transferrin and non-transferrin-bound-iron by deferiprone. Implications in the treatment of thalassemia, anemia of chronic disease, cancer and other conditions. Hemoglobin 2006;30:183–200.
6. Deschauer M, Gaul C, Behrmann C, et al. C19orf12 mutations in neurodegeneration with brain iron accumulation mimicking juvenile amyotrophic lateral sclerosis. J Neurol 2012;259:2434–2439.
7. Schweser F, Deistung A, Lehr BW, Reichenbach JR. Quantitative imaging of intrinsic magnetic tissue properties using MRI signal phase: an approach to in vivo brain iron metabolism? NeuroImage 2011;54:2789–2807.
8. Robinson S, Grabner G, Witoszynskyj S, Trattnig S. Combining phase images from multi-channel RF coils using 3D phase offset maps derived from a dual-echo scan. Magn Reson Med 2011;65:1638–1648.
9. Abdul-Rahman HS, Gdeisat MA, Burton DR, et al. Fast and robust three-dimensional best path phase unwrapping algorithm. Appl Opt 2007;46:6623–6635.
10. Wu B, Li W, Avram AV, et al. Fast and tissue-optimized mapping of magnetic susceptibility and T2* with multi-echo and multi-shot spirals. NeuroImage 2012;59:297–305.
11. Schweser F, Sommer K, Deistung A, Reichenbach JR. Quantitative susceptibility mapping for investigating subtle susceptibility variations in the human brain. NeuroImage 2012;62:2083–2100.
12. Rorden C, Brett M. Stereotaxic display of brain lesions. Behav Neurol 2000;12:191–200.
13. Sedlacik J, Boelmans K, Lobel U, et al. Reversible, irreversible and effective transverse relaxation rates in normal aging brain at 3T. NeuroImage 2013;84C:1032–1041.

14. Hallgren B, Sourander P. The effect of age on the non-haemin iron in the human brain. J Neurochem 1958;3:41–51.
15. Langkammer C, Schweser F, Krebs N, et al. Quantitative susceptibility mapping (QSM) as a means to measure brain iron? A post mortem validation study NeuroImage 2012;62:1593–1599.
16. Aquino D, Bizzi A, Grisoli M, et al. Age-related iron deposition in the basal ganglia: quantitative analysis in healthy subjects. Radiology 2009;252:165–172.
17. Schweser F, Sedlacik J, Deistung A, Reichenbach JR. Non-invasive Investigation of the Compartmentalization of Iron in the Human Brain. ISMRM 21st Annual Meeting & Exhibition. Salt Lake City, Utah, 2013; p. 0460.
18. Ziener CH, Bauer WR, Jakob PM. Transverse relaxation of cells labeled with magnetic nanoparticles. Magn Reson Med 2005;54:702–706.
19. Hogarth P, Gregory A, Kruer MC, et al. New NBIA subtype: genetic, clinical, pathologic, and radiographic features of MPAN. Neurology 2013;80:268–275.
20. Kruer MC, Hiken M, Gregory A, et al. Novel histopathologic findings in molecularly-confirmed pantothenate kinase-associated neurodegeneration. Brain 2011;134(Pt 4):947–958.

Supporting Information

Additional Supporting Information may be found in the online version of this article:

Figure S1. Electron microscopy of skin biopsy showing mitochondrial degeneration in endothelia of a small vessel (lower box in overview and lower left image) and a mitochondrion with intact cristae (upper box in overview and lower right image). Note: en, endothelial cell; ec, erythrocyte.

Table S1. Mean values and standard deviation (over all voxels in corresponding ROI) for R2, R2*, and quantitative susceptibility mapping (QSM) and estimated brain iron content of our patient over a period of 24 months under iron-chelating therapy.

